Review of necessary thermophysical properties and their sensivities with temperature and electrolyte mass fractions for alkaline water electrolysis multiphysics modelling

Damien Le Bideau, Philippe Mandin, Mohamed Benbouzid, Myeongsub Kim, Mathieu Sellier

Review of necessary thermophysical properties and their sensivities with temperature and electrolyte mass fractions for alkaline water electrolysis Multiphysics modelling

Damien Le Bideau[(1)], Philippe Mandin[(1)*], Myeongsub Kim[(2)], Mathieu Sellier[(3)]

[(1)] Université Bretagne Sud, IRDL UMR CNRS 6027, 56100 Lorient, France

[(2)] Department of Ocean and Mechanical Engineering, Florida Atlantic University, Boca Raton, USA

[(3)] Department of Mechanical Engineering, University of Canterbury, Christchurch 8140, New Zealand

[*] Corresponding author, philippe.mandin@univ-ubs.fr

Abstract

This article presents an exhaustive review of the transport properties necessary for the multiphysics modelling of alkaline water electrolyzer. This article provides experimental data and the correlations needed to calculate thermos-physical properties such as electrical conductivity, density, viscosity, heat capacity, heat and mass transfer diffusion coefficients as a function of temperature and electrolyte mass fraction for two classical alkaline electrolytes (KOH, NaOH). Thus, the different boundary layers growing on the electrodes can be calculated with precision. Different interpolation models from various authors are compared to raw experimental data. The goal of this article is to give to the modeler the correlations needed for the simulation of alkaline water electrolysis.

Keywords

Alkalin electrolysis, multiphysics modelling, electrolyte, thermophysical properties

Nomenclature

Roman symbol

a	Heat diffusivity ($m^2 s^{-1}$)
c	Species molar concentration ($mol\ m^{-3}$)
Cp	Specific heat ($J\ kg^{-1}\ K^{-1}$)
D	Species diffusion coefficient ($m^2 s^{-1}$)
g	acceleration constant
h	Heat convection coefficient ($W\ m^{-2}\ K^{-1}$)
I	Intensity (A)
j	Current density ($A\ m^{-2}$)
k	Mass transfer coefficient ($m\ s^{-1}$)
M	Molar mass ($kg\ mol^{-1}$)
n	species quantity (mol)
J	Mass flux density ($mol\ m^{-2}\ s^{-1}$)
P	Power (W)
R	Electrical resistance (Ω)
r_m	atomic radius (Å)
S	Surface area (m^2)
T	temperature (°C)
t	time (s)
V	velocity ($m\ s^{-1}$)
U	Electrical imposed potential (V)
U	Vector velocity
X	species molar fraction (-)
Y	species mass fraction (-)
x, y, z	Spatial coordinates (m)

Greek symbol

α	Wang's coefficient (-)
λ	heat conductivity ($W\ m^{-1}\ K^{-1}$)
ρ	density ($kg\ m^{-3}$)
μ	Dynamic viscosity ($kg\ m^{-1}\ s^{-1}$)
η	Over potential (V)
σ	Electrical Conductivity ($S\ m^{-1}$)
ν	Kinematic viscosity ($m^2 s^{-1}$)
ϕ	electrical potential (V)

Subscripts

a	anode
act	activation
av	average
c	cathode
conc	concentration
i	species
l	limit
r	reactions

Constants

R	Ideal gas constant = $8{,}314\ J\ mol^{-1}\ K^{-1}$
F	Faraday's constant = $96485\ C\ mol^{-1}$

1 Introduction

The challenge of the 21st century is to decrease CO_2 emission in order to manage and decrease global warming. The main solution to this problem is to produce energy from renewable energy and if possible without the help of hydrocarbon and carbon molecules. Due to the fact that renewable

energies are intermittent in space and time, current production cannot be integrated properly on the electrical network. From this statement, one deduces that energy must be stored in small or medium scale smart grids. Electrical networks are not designed to receive renewable production and it is not always possible (isolated locations, islands, mountains, full sea…). In these cases, it is necessary to store the electricity produced.
The social and economic decarbonation new challenges might give a great place to hydrogen energy. Because hydrogen species are not produced naturally, it will be necessary for storage or mobility challenges to define a new decarbonated hydrogen production process: the electrolysis instead of actual methane cracking.
Alkaline water electrolyzers are the more extensively used for massive hydrogen production. Nevertheless, it appears two new and interesting alternantive processes. The first one is the proton exchange membrane electrolyzer (PEME). It is with greater performances but involves platinum and membranes which make the cost more expensive and with less robustness. The second is the solide oxide electrolyzer (SOE). This hot temperature technology consuming directly water vapor is always in evaluation in laboratories.
Both are based on the fuel cell material studies and adapted to electrolyzer process.

The present study is placed in this context. Using hydrogen as an energy vector could solve this issue because its production only requires H_2O and electricity or light. However, the cost of hydrogen production (alkaline, acid, thermochemical combined cycles or high temperature) is too high compared fuel, gasoil, or electrical energy produced with nuclear or thermal plants. Presently, electrolysis or photocatalytic ([1], [2]) processes are not efficient or cheap enough and they must be optimized. Alkaline water electrolysis is the oldest process, the most robust and cheapest technology. It has been studied theoretically and experimentally for a long time but most of the theoretical studies are primary or secondary charge transfer modelling (charge transfer modelling with activation overpotentials considered). These works do not take into account the local temperature and hydroxide; moreover, electro-active species such as hydroxide ions (OH^-) are not calculated. Modern technologies allow us to investigate and improve the electrolysis by using Computational Fluid Dynamics (CFD) modelling, under ternary assumptions. CFD models allow one to access current density distribution at electrodes for example. This modelling goal needs at least six liquid electrolyte parameters:
1/ electrical conductivity σ (S m^{-1}),

2/ density $\rho(T,Y)$ (kg m^{-3}) ,

3/ viscosity $\mu(T,Y)$ (kg m^{-1} s^{-1}),

4/ specific heat $Cp(T,Y)$ (J kg^{-1} K^{-1}),

5/ thermal conductivity $\lambda(T,Y)$ (W m^{-1} K^{-1}),

6/ mass transfer diffusion coefficient $D(T,Y)$ (m^2 s^{-1}).

These thermos-physical properties are dependent on the local electrolyte mass fraction Y (-) and temperature T (K). The first step in the modelling exercise involves obtaining all the input properties and their sensitivity to temperature and electrolyte mass fraction. The present gives a complete and exhaustive review of these parameters and provide accurate correlations ready to implement for modelers.
The complete set of thermophysical properties for alkaline water electrolyzers multiphysics modelling: electrical conductivity, density, viscosity, heat capacity, thermal conductivity and hydroxide ions diffusivity is given. These properties sensitivities with pressure and temperature levels and also with alkaline species concentration. This complete set of data allow future rigorous

calculation of triple two-phase boundary layers at both alkaline water electrolyzer electrodes. This will allow better primary, secondary or ternary current distribution modelling at both electrodes. It also allows multi scale calculation at both bubbles and electrolyzer scales with appropriate input data. The knowledge of thermophysical properties discrepancies among different authors allows uncertainty evaluations on electrolyzer performances.

Few studies describe one or two parameters but none provides the 6 parameters cited above and their sensitivities. Of particular interest to the present review is the work of Zaytsev et al.[3] which provides a partially complete collection of several data and their sensitivities, sometimes obtained experimentally or calculated with molecular dynamics simulations. However, this reference which is a general handbook for aqueous dissolved salts data is hardly accessible, expensive and contains much unnecessary data for irrelevant salts for the alkaline water electrolysis process. Also, Zaytsev et al.[3] does not give all the necessary data and corresponding fitting correlations. The electrical conductivity σ (S m^{-1}) and mass transfer diffusion D (m^2 s^{-1}) coefficients are missing, for example. Table 1 presents all the references used to write the present review. Much of the reference data come from Zaytsev et al. handbook[3] but also from See et al for KOH electrical conductivity[4], Mashovets et al[5] for KOH density, Hitchcock et al[6] for KOH viscosity. For NaOH, Kreys [7] is used for NaOH density. For NaOH conductivity, Maksimova et al is used[8]. For NaOH viscosity, Krings et al is used[9]. Gilliam et al.[10] was used for the electrical conductivity σ (S m^{-1}) and the density of KOH. See and White[4] also give data and correlation but only for the electrical conductivity σ (S m^{-1}). The electrical conductivity is widely available in previous literature on alkaline water electrolysis because this property is a key parameter and the only necessary one for the simplest modelling (primary or secondary current density distribution, for example). Klochko and Godneva[11] also reported few points for the KOH and NaOH electrical conductivity σ (S m^{-1}) and viscosity μ (kg m^{-1} s^{-1}). Guo et al.[12] provides correlations and experimental data for KOH density ρ (kg m^{-3}) and viscosity μ (kg m^{-1} s^{-1}). Laliberté[13] and Roux et al.[14] present a method to determine correlations for KOH and NaOH density ρ (kg m^{-3}), viscosity μ (kg m^{-1} s^{-1}) and specific heat Cp (J kg^{-1} K^{-1}) from experimental data. Wang and Anderko[15] and Riedel[16] work was used for the KOH and NaOH thermal conductivity λ(W m^{-1} K^{-1}) correlations. Three mains articles (Akerlof and Kegeles[17], Olsson et al.[18], and Churikov et al. [19]) describe the NaOH density ρ (kg m^{-3}). Ref.[18] also supplies correlations and data for NaOH viscosity μ (kg m^{-1} s^{-1}). Lobo et al compiled the aforementioned experimental data for electrical conductivity, density, viscosity[20]. The more difficult to find was the diffusion coefficient D (m^2 s^{-1}) and its dependence on the temperature T and electrolyte mass fraction Y (-) for OH^- hydroxide anions at anode which is essential data for ternary modelling of current density distribution. This is due of the small number of published studies under this ternary modelling assumption. It was more difficult to find for NaOH instead of KOH. We have developed a correlation with the little data available.

Table 1 around here

2 Electrolysis working point and Thermodynamics

To choose the right nominal point, thermochemistry theory is first invoked. The desired hydrogen production of the alkaline electrolyzer N_{H2} (mol m^{-2} s^{-1}) and the electrical power P (W) consumed depend on the imposed potential U (V) of the cell, the average current density j_{av} (A m^{-2}) and the

total surface electrolyzer area S (m^2). The following points are important to consider for hydrogen production by alkaline electrolysis:

1/ The larger the average current density j_{av} (A m^{-2}), the larger the hydrogen production. This fact results from faraday law (1):

$$N_{H2} = j_{av}\, n_e^{-1}\, F^{-1} \quad (1)$$

With N_{H2} the molar flux in mol m^{-2} s^{-1}, n_e (mol) the electrons number that is exchange during the electrolysis process and F the Faraday constant.

2/ The smaller the cell imposed potential U (V), the cheaper the hydrogen production. This fact is formalized by the potential equation:

$$U_{cell} = E_{rev} + \eta_{ohm} + \Sigma\eta_{act}(j) + \Sigma\eta_{conc}(j) \quad (2)$$

1^{st} 2^{nd} 3^{rd}

With E_{rev} (V) the reversible potential, η_{act} and η_{conc} the activation and concentration overvoltage in Volt, respectively. 1^{st} stands for primary charge modelling, 2^{nd} for secondary charge modelling and 3^{rd} the ternary charge modelling (Figure 1).

Figure 1 around here

Consequently, for massive and cost-effective hydrogen production, the intensity must be as large as possible, and the applied cell potential must be the lowest. However, the consumed potential increases with the average current density j_{av} applied to the cell. The cell imposed potential is consumed by 3 processes (equation 2):

1/ The reversible tension and the ohmic drop defines the primary consumption;

2/ The addition of the activation overpotential at anode and cathode constitutes the secondary consumption;

3/ The addition of the concentration and bubbles effects over potential is the ternary consumption.

This last consumption is particularly important for large average current density electrolyzer and critical due to the limiting hydroxide anions flux (N_{OH} in mol m^{-2} s^{-1}), Oxygen Evolution Reaction (OER) at anode, and Hydrogen Evolution reaction (HER) at cathode. The birth, growth and departure of bubbles lead to a lower effective electro-active surface due to screening effect quantified with θ (-). The bubbles also change the effective two-phase thermophysical properties according to the gas bubbles void fraction ε (-).

Each overvoltage needs optimization. Historically, the reversible potential is optimized, then the Ohmic drop and after the activation overvoltages … the concentration overoltages are not yet optimized for many electrochemical systems because they need flow optimization which is our final goal.

The present part focuses on the reversible tension because this one depends on the thermodynamics. Olivier et al.[21] proved that the reversible tension decreases with increasing temperature. The constraint is the boiling point because vapor bubbles are less conductive than the liquid electrolyte and the appearance of more bubbles triggers a new overpotential off. For a good electrolyzer design, the goal is to stay under this boiling point. In [21], the authors also proved that the reversible tension slightly increases with an increasing pressure. However, the increase is small and the higher the pressure, the smaller the bubbles and the better the storage of produced hydrogen. The following describes how various parameters depend on pressure:

- The electrical conductivity of electrolytes increases with pressure according to Hamann et al[22] and Gancy et al [23]. Hamann et al say that the conductivity of KOH increases by 29% between 1 bar and 75000 bar. Gancy et al [23] proved that the electrical conductivity of aqueous KCl increases by about 15% between 1 bar and 2000 bar at a temperature of 5°C and less than 1% at a temperature of 85°C. In addition, knowing that the maximum operating pressure for an electrolyzer is 200 bar and the temperature is about 80°C, we can assume that the electrical conductivity is not depending on pressure.
- Water is often considered incompressible. In fact, its density increases by 2% in average between 1bar and 200 bar for all temperatures. In addition, Fine et al[24] proved that the compressibility factor is 10^{-6} bar^{-1} which is 10^{6} less than the compressibility of air.
- The effect of pressure on viscosity is not negligible between 1 and 200 bar as the viscosity of the water is multiplied by 100000 according to Le Neindre[25]. According to Schmelzer et al [26], the viscosity of water follows an inverse parabolic curve below 33°C.
- We have seen that water can be considered incompressible so the specific heat can be taken as constant and therefore independent of pressure.
- For the thermal conductivity of the aqueous electrolyte, Le Neindre's[27] work reports that the thermal conductivity of water increases by only 8% (in average) for all the temperature between 110MPa and 250MPa and 3% from 0.1MPa to 110MPa.

Figure 2 around here

The following set of equation(eq(3) to eq(8)) are taken from Zaytsev [3]. Eq(3) and Eq(4) are correlation that correlate the boiling point to the KOH or NaOH mass fraction. Those correlations show that the boiling point increases with an KOH mass fraction increase.

Boiling point

For KOH: $T_b(Y) = -5.933\,10\,Y^3 + 1.756\,10^2\,Y^2 + 5.533\,Y + 9.995\,10^1$ (3)

For NaOH : $T_b(Y)= -3.92\ 10^2\ Y^3 + 3.214\ 10^2\ Y^2 - 9.395\ 10\ Y + 1.005\ 10^2$ (4)

The eq(5) and eq(6) correlate the saturated pressure of KOH electrolytes for two mass fractions. The eq(7) and eq(8) correlate the saturaded pressure of NaOH electrolytes for two mass fractions. For both KOH and NaOH, an increasing temperature increases the saturaded pressure.

Saturated pressure

KOH Y=0.3 $Ps(T)= 1.763\ 10^{-6}\ T^3 – 1.633\ 10^{-4}\ T^2 + 5.460\ 10^{-3}\ T – 2.124\ 10^{-2}$ (5)

KOH Y=0.36 $Ps(T)= 1.479\ 10^{-6}\ 10^{-3}\ T^3 – 1.400\ 10^{-4}\ T^2 + 4.635\ 10^{-3}\ T – 1.862\ 10^{-2}$ (6)

NaOH Y=0.15 $Ps(T)= 2.143\ 10^{-6}\ T^3 – 1.843\ 10^{-4} T^2 + 6.103\ 10^{-3}\ T - 2.162\ 10^{-2}$ (7)

NaOH Y=0.25 $Ps(T)= 2.003\ 10^{-6}\ T^3 – 1.880\ 10^{-4}\ T^2 + 6.062\ 10^{-3}\ T - 1.822\ 10^{-2}$ (8)

3 Comparison tool

In this study, several models and fitted correlations have been analyzed and compared to experimental data. To help the reader, this part will explain how the comparison was performed. To compare the correlations with the data, the following equation was used:

$$\Delta A=(A_{Zaytsev}-A_{correlation})\ 100/A_{Zaytsev} \quad (9)$$

$A_{Zaytsev}$ an experimental value of a parameter in SI units from Zaytsev. $A_{correlation}$ a value obtained from a correlation. A can be substituted by ρ, λ, σ, Cp etc. Then the following equations have been used to compare correlation and model:

$$\Delta A_{av}=\Sigma\Delta A/N \quad (10)$$

With N the number of ΔA evaluated.

The above relation gives the average errors percentage over a temperature and mass fraction range.

$$\Delta A_{max}=\max(\Delta A) \quad (11)$$

Eq. (11) gives the maximum errors percentage over a temperature and mass fraction range.

Figure 3 around here

Figure 3 shows graphically what are ΔA_{av} and ΔA_{max}.

4 Charge transfer: electrical conductivity

The simplest model to simulate the water electrolysis is a model which just calculates the potential gradient over the cell. It is a one-dimensional model that solve the electric potential equation.

$$\nabla\cdot(\sigma\ \nabla\ \varphi)+S=0 \quad (12)$$

Only one parameter is needed in this case: the electrical conductivity. This model gives a first approximation of the pair U, j but does not consider the motion of the electrolyte or the concentration of OH^-. The corresponding electrolysis model is the Ohmic model is given by:

$$U_{cell} = E_{rev} + \eta_{ohm} + \Sigma\eta_{act}(j) \quad (13)$$

In this part, the molarity will be used to calculate the electrical conductivity. The equation used to calculate this molarity is given by:

$$C = Y_{KOH}\, \rho_{KOH}\, M_{KOH}^{-1} \quad (14)$$

Y the mass fraction of KOH in the electrolyte, ρ_{KOH} the density of the electrolyte in kg m^{-3}, M_{KOH} the molar mass g mol^{-1} and C is in mol L^{-1} or M.

4.1 KOH

For the KOH electrical conductivity, the data was taken from Zaytsev [3] and the correlations from [4] and Gilliam et al [10]. In Zaytsev [3], the electrical conductivity is available between 0 and 70°C and 0-0.48 of KOH mass fraction. It can be noticed that Klochko et al[11] supply few data points for electrical conductivity in [4]. All the authors agree on the evolution of the conductivity with temperature and KOH mass fraction. Indeed, the electrical conductivity increases linearly with the temperature and reaches a maximum before decreasing with an increasing KOH mass fraction. This maximum is reached between 0.28 (T<10°C) and 0.32 (60°C<T<70°C) in KOH mass. In Allebrod et al[28], the authors report that for a temperature greater than 100°C, the maximum is greater than 0.375 KOH.

4.1.1 Gilliam equation

Gilliam [10] used a set of experimental data obtained from other sources (see [4]) and from their own experiments. Then the authors developed the following empirical correlation using a non-linear regression. The correlation is valid for temperature between T in [0-100°C] and Y_{KOH} in [0.01-0.48].

$$\sigma = -K_1\, C - K_2\, C^2 + K_3\, C\, T + K_4\, C\, T + K_5\, C^3 - K_6\, C\, T^2 \quad (15)$$

with Y the KOH mass fraction, T the temperature in K, and σ the electrical conductivity of the electrolyte in S m^{-1}.

4.1.2 See and White equation

The See correlation was developed from See's experimental data [2]: 0.15-0.45 mass fraction KOH, -15-100°C. As Gilliam et al[10], the author(s) uses a non-linear regression which results in

$$\sigma = K_1\, Y_{KOH} + K_2\, T + K_3\, T^2 + K_4\, T\, Y_{KOH} + K_5\, T^2\, Y_{KOH}^{K6} + K_7\, T\, Y_{KOH}^{-1} + K_8\, Y_{KOH}\, T^{-1} \quad (16)$$

$Y_{KOH}$is the KOH mass fraction and T the temperature in K.

4.1.3 Current study equation

Gilliam[3] and See's equation [4] are good model but the author propose a simpler correlation in order to provide a simple equation easy and quick to enter in calculator device. A simple correlation which predicts the electrical conductivity has been developed using a nonlinear GRG minimization method.

$$\sigma = K_1 + K_2\, T + K_3\, Y_{KOH}^2 + K_4\, Y_{KOH}^3 + K_5\, T\, Y_{KOH} \quad (17)$$

This model is accurate with an averaged error of 3.34% between T=[40-70°C] and Y_{KOH}=[0.16-0.32]

4.1.4 Comparison with data

The comparison with See's correlation[4] gives an average difference of 5.36% and a maximum of 11.58% in the range T in [40;70] °C and Y_{KOH} in [0.02;0.40]. The maximum difference is 11.58%. In this range, there are only two points more than 10% apart, they are both at 40°C with a mass fraction of 0.22 and 0.24. For the Gilliam's correlation [3], an average difference of 4,12% is obtained with of maximum of 10,58%. The two points above 10% are the same as those observed for See's correlation. Current study model is simpler to use than the other but is restricted to the range Y_{KOH} in [0.16;0.32] and T in [40;70°C]. In this range, the average difference is 3.34% with a maximum reached at T=40°C and Y_{KOH}=0.16 of 18.83%. The correlations for KOH conductivity have also been compared to See and White's data. See correlation's has an average difference of 1.25% and a maximum difference of 7.40%. Gilliam's equation has an average difference of 3.04% and a maximum difference of around 14% with See and White data. The current study correlation fit less than with Zaytsev data (15% of average difference). The results of the comparison and the value of the parameters are presented in the table 2.

Table 2 around here

4.2 NaOH

Zaytsev [3] gives experimental data but unfortunetly no correlation could be found to describe the evolution of NaOH with temperature and mass fraction. We developed here a correlation using the least square method. Zaytsev [3] gives data from 0 to 50°C and Y_{NaOH} in [0;0.25]. According to Zaytsev[3], the evolution of the electrical conductivity of aqueous NaOH is the same as aqueous KOH but the maximum is reached Y_{NaOH} in [0.16;0.20]. The designed correlation uses data between T in [35;50]°C and Y_{NaOH} in [0.08;0.3]. The corresponding equation is:

$$\sigma = K_1 + K_2\, T + K_3\, Y_{NaOH}^{3} + K_4\, Y_{NaOH}^{2} + K_5\, Y_{NaOH} \qquad (18)$$

This correlation applied over the the range Y_{NaOH} in [0;0.25] and T in [0;50] °C, the average difference is 1.5% with a maximum of 11.7% at 50°C and 0.08 NaOH mass fraction. However, the correlation fit with a difference of 20% with Maksimova's data.

Figure 4 around here

5 Momentum transfer

The calculation of the momentum conversation equation becomes necessary in the case of the ternary charge distribution. Indeed, species distribution is dependent on the electrolyte flow. The flow is computed using the continuity and momentum conservation (the Navier-Stokes equations eq(19) and continuity equation eq. (20) which allow the calculation of the pressure and velocity field. Two parameters are needed here: the density and viscosity.

$$\rho\, d\mathbf{U}/dt + \nabla\cdot(\rho \mathbf{U}\, \mathbf{U}) = -\nabla p + \nabla\cdot\tau + \rho \mathbf{g} \qquad (19)$$

$$\nabla\cdot(\rho\, \mathbf{U}) = 0 \qquad (20)$$

5.1 Density

For both NaOH and KOH, the results of the review and the comparison with experimental data are presented in the table 3.

5.1.1 Zaytsev Model

Zaytev[1] used the pycnometric method to determine the density of the two aqueous electrolyte up to 90°C . Then, two correlations were used to extrapolate the results up to 200°C.

For both KOH and NaOH Zaytsev [3] uses the same correlation given by:

$$\rho = (K_1 + T\, K_2 + K_3\, T^2)\; 10\text{^}((\, K_4 + K_5\, T)\, Y_i)) \qquad (21)$$

5.1.2 KOH

For the KOH, data between T in [0;200] °C and Y_{KOH} in [0;0.50] KOH are available in Zaytsev [3]. Those data will be compared to correlations from Zaytsev [3] eq. (21) Gilliam et al[10] eq. (22). The sensitivity of the density to the temperature between 0 and 105°C oscillate around -0.5 kg m^{-3} K^{-1}.

This value varies between -0.47 kg m^{-3} K^{-1} (at 2% KOH) and -0.68 kg m^{-3} K^{-1}. In comparison, the sensitivity to the mass fraction is around 10 kg m^{-3} $\%_{KOH}^{-1}$and it is independent of temperature. To sum up, the density decreases slowly with temperature but increases rapidly with mass fraction. The two evolutions are almost linear. The two correlations give satisfactory results compared to Zaytsev's data (less than 1% of difference) and less than 3% compared to Mashovet's data.

5.1.2.1 Gilliam model

Gilliam et al[10] used the dataset from Zaytsev [3] and others ([11], [29]) to develop a correlation of density. In this work, the authors choose to use the following form:

$$\rho = \rho_{water} \exp(K_4 Y_{KOH}) \quad (22)$$

with K the value of the water density for one specific temperature. In order to facilitate the use, the factor K has been replaced by a temperature-dependent quadratic polynomial according to eq. (20).

$$\rho = (K_1 T^2 + K_2 T + K_3) \exp(K_4 Y_{KOH}) \quad (23)$$

T the temperature in °C, Y the KOH mass fraction, ρ in kg m^{-3}.

5.1.3 NaOH

Zaytsev [3] gives data for density of NaOH form 0°C to 200°C and Y_{NaOH} in [0;0.40]. The sensitivity with temperature of the density of aqueous NaOH is a little bit smaller than the KOH's aqueous density (-0.78 kg m^{-3} K^{-1} but the progression goes from -0.6 to -1.1 kg m^{-3} K^{-1} from 0.02 to 0.30). The sensitivity with mass fraction is almost the same as KOH's sensivity with mass fraction (17.4 kg m^{-3} $\%_{NaOH}^{-1}$), almost linear for both temperature and mass fraction. The two selected model has been developed by Zaytsev eq. (21) [3] and Churikov [19] eq. (24).

5.1.3.1 Churikov model

First, Churikov [19] has performed pycnometry to measure the density of NaOH, then he used identification to determine the coefficient of the following model:

$$\rho = K_1 + K_2 T + K_3 T^2 + (K_4 Y^2 + K_5 Y) \quad (24)$$

T the temperature in °C, Y the KOH mass fraction, ρ in kg m^{-3}.

5.1.3.2 Comparison with experimental data

The correlation given by Zaytsev [3] is very accurate for high NaOH concentration (0.54% difference for T in [60-105°C] and Y_{NaOH} in [0.02;0.30] with a maximum of 0.66% for 100°C and Y_{NaOH}=0.3). Churikov's correlation [19] gives satisfactory results for low and high concentration of KOH (1% of difference in average for T in [60;105] °C and Y_{NaOH} in [0.02;0.40] with a maximum of 4%). Krey's data has also been used to compared the correlations[7]. Zaytsev's correlation has 2% of average difference with a maximum difference of 6.8% and Churikov's correlation has 0.6% of average difference with a maximum difference of 1.5% for T in [60;100]°C and Y_{NaOH} in [0.10;0.50].

5.1.4 Multilinear interpolation

For both electrolyte models a correlation was developed using experimental data of Zaytsev. Those models are easy to use and since the evolution with the temperature and mass fraction is quasilinear, the models is valid and given by:

$$\rho(Y_i,T) = K_1 + K_2 Y_i + K_3 T + K_4 T Y_i \quad (25)$$

where T the temperature in °C, Y_i the KOH mass fraction.The constants are reported in Table 3.

Table3 and Figure 5 around here

5.2 Viscosity

For both NaOH and KOH, the results of the review and the comparison with experimental data are presented in the table 6. The Olsson correlation is presented two other table. Table 4 gives the coefficient values and table 5 gives the domain of validity.

5.2.1 Zaytsev model

Zaytsev [3] collected data for the viscosity of both electrolytes from other scientists. From those data, the author determined two correlations (one for the isotherms and one for the isomasses) and extrapolated the data from 90°C to 200°C leading to the following correlation:

$$\mu=(K_1 (K_2 +T) - K_3 + 10\text{^}((K_4 + K_5 T) Y)))\times 10^3 \quad (26)$$

T the temperature in °C, Y_i the mass fraction, μ in mPa s.

The values of the correlation parameter are presented in Table 6.

5.2.2 KOH

5.2.2.1 Guo's model

The following model was firstly designed for the ternary electrolyte system K_2CrO_4-KOH-H_2O. The empirical model eq. (27) was determined using capillary viscometer data. The measurements were taken in the range 15 to 60°C.

$$\mu= \exp(K_1 + K_2 T + K_3 T^2 + K_4 C) \quad (27)$$

T the temperature in °C, M_{KOH} the molar mass of KOH in g mol^{-1}; Y_{KOH} the mass fraction, μ in mPa s.

5.2.2.2 Analysis and comparison with experimental data

The available data in Zaytsev's books [3] are in the range T=[0-200]°C and Y_{KOH}=[0-0.50]. The viscosity decreases exponentially with the temperature whereas it increases exponentially with the mass fraction. To model this evolution, two models have been chosen: Zaytsev's model [3] eq. (26) and Guo's model [12] eq. (27). Zaytsev's correlations [3] describes the evolutions in mass fraction and temperature with an average difference of 2.9%, a maximum of difference of 18% at 60°C and Y_{KOH}=0.40 of mass. Guo's model [12] has an average difference with Zaytsev [3] of 5% for temperature between 20-60°C and mass fraction between Y_{KOH} in [0;0.40] KOH but for temperature greater than 60°C a divergence is observed (10% of difference for all the mass fraction). Due to the high departure from linearity of the viscosity evolution and the availability of correlations to describe this evolution, no additional model was developed. Two set of data has been used for the viscosity. Zaytsev's data and Hitchcock's data. Using this two sets, Guo's correlation is the best correlation because its average difference with the two set of data is around the average difference of Zaytev's correlation and the maximum difference is less than Zaytsev's correlation.

5.2.3 NaOH

5.2.3.1 Olson model

Olsson [18] collected data from other studies and used them to make a correlation of viscosity correlated with temperature and mass fraction. The correlation is reported below with the corresponding parameters in Table 4:

$$\mu = (10\text{^}(\log_{10}((\ 5.98\ 10^{-1}\ (4.32\ 10^{1} + T) - 1.54\ )) + (\ 3.39 - 1.12\ 10^{-2}\ \ T)\ Y))\ 10^{3} \quad (28)$$

$$\ln(\mu_{NaOH}/\mu_{H2O}) = d_1 + d_2\ T^{1/2} + d_3\ T \quad (20)$$

$$d_1 = k_1\ Y_{NaOH} + \ldots + k_4\ Y_{NaOH}^{\ 4}$$

$$d_2 = l_1\ Y_{NaOH} + \ldots + l_5\ Y_{NaOH}^{\ 5}$$

$$d_3 = m_1\ Y_{NaOH} + \ldots + m_5 YNaOH5$$

$$\mu_{H2O} = \exp(\ n_0 + n_1\ T + n_2\ T^{1.5} + n_3\ T^{2,5} + n_4\ T^{3}\ )$$

This correlation can be used only in the intervals reported in Table 5.

Table 4 and Table 5 around here

5.2.3.2 Comparison with experimental data

For NaOH, data is available in Zaytsev [3] between 0 and 200°C and 0-0.50 of mass fraction. The two models are Zaytsev's eq. (26) and Olsson's model eq. (28). The Zaytsev's model [3] has an average difference of 5% whereas Olson's is 6% over the range T in [60;105°C] and Y_{NaOH} in[2;0.40]. Also, for Olsson's correlation the difference reaches 15% at 100°C. This model has the particularity to have an interval of validity depending on mass fraction. This domain of validity is presented in the Table 5.

Table 6 and Figure 6 around here

6 Heat transfer

The calculation of heat equation can bring more precision on the calculation of the pressure and velocity fields and can also influence species transport. Indeed, a temperature gradient triggers natural convection and most of the parameters are temperature dependent. To calculate the temperature field, three parameters are needed: density, specific heat, thermal conductivity. The two first are necessary generally in time dependent studies because they characterize the inertia of the system. The last one is needed for both stationary and time-dependent studies. The eq(29) is the general energy equation.

$$\rho\ Cp\ dT/dt + \rho\ Cp\ \nabla \cdot UT = \Delta(\lambda\ T) + P \quad (29)$$

6.1 Specific heat

For both NaOH and KOH, the results of the review and the comparison with experimental data are presented in the table 7.

6.1.1 Zaytsev model

The experimental method used by Zaytsev [3] to get data is:

- For KOH, the author used an isothermal glass calorimeter then used the same technique of extrapolation as for the other parameters.
- For NaOH, the author collected data from other scientists and extrapolated extrapolated them.

The same model is used by Zaytsev [3] to describe the evolution of specific heat for NaOH and KOH. This model is described by the equation below:

$$Cp = K_1 + K_2 \ln(T/100) + (K_3 + K_4 Y + 8 T) Y_i \quad (30)$$

with T the temperature in °C and Y the mass fraction.

6.1.2 Method of Lalibertée

Laliberté [13] use the following equation to model the specific heat of the KOH and NaOH. In his article, Laliberté [13] explain how to use his method. First, experimental must be collected then initial coefficient must be chose. The squared difference between the experimental and model data is made and this difference gives a criterion to minimize using a solver.

$$Cp = Y_i (K_1 \exp(\alpha) + K_5 Y_i^{K6}) + (1-Y_i) Cp_{water} \quad (31)$$

$$\alpha = K_2 T + K_3 \exp(0.01 T) + K_4 Y_i \quad (32)$$

6.1.3 Multilinear interpolation

The experimental and extrapolated values of Zaytsev has been used to create this interpolation eq. (33).

$$Cp(Y_i,T) = K_1 + K_2 Y + K_3 T + K_4 T Y_i \quad (33)$$

with T the temperature in °C and Y the mass fraction.

Due to the quasi linearity of the specific heat evolution with temperature and mass fraction a bilinear interpolation has been fitted. The table 7 gives the corresponding parameters to use and the domain of validity.

6.1.4 Comparison with experimental data: KOH

The study of the temperature sensitivity shows that the evolution with temperature of the specific heat is cubic because the derivative with respect to temperature of the specific heat with respect to the temperature increases slighty before decreasing (the average increase and decrease is in average around ± 3 kJ kg^{-1} K^{-2}). The sensitivity with respect to temperature is negligible compared to that with respect to the mass fraction which decreases linearly with a slope of -33 kJ kg^{-1} $K^{-1}\%_{KOH}^{-1}$. Two models have been selected: Zaytsev's model eq. (30) [3] and Laliberté's eq. (31) and eq. (32) model [13]. Zaytsev's model eq. (30) [3] has an accuracy of 2% on average in the range Y_{KOH} in [0-0.40] KOH and 0-100°C with a maximum of 8%. Laliberté's model [13] is accurate at 1.1% in the range [0-0.40] KOH mass fraction and 60-100°C with a maximum of 2.58% at 0.08 KOH mass fraction and 60°C.

6.1.5 Comparison with experimental data: NaOH

In his book, Zaytsev [3] gives NaOH specific heat data from 0 to 200°C and Y_{NaOH} in [0;0.42]. The correlation given by Zaytsev [1] has an average difference of 2% with a maximum of 4.32% at 90°C and 20% NaOH. The identification method of Laliberté [13] was used to get another model, the same

problem as for KOH can be observed. This model is valid between 60 and 100°C. The average difference is around 1.72% with a maximum of 6.16% for 60°C and Y_{NaOH}=0.42.

Table 7 and Figure 7 around here

6.2 Thermal conductivity

For both NaOH and KOH, the results of the review and the comparison with experimental data are presented in the table 8.

6.2.1 Zaytsev model

Zaytsev [3] has selected data from other scientists and then used the same method as before to extrapolate the results. Accordingly,

$$\lambda = (K_1 + K_2 T - K_3 T^2) (1-Y_i K_4) \quad (34)$$

6.2.2 Wang model

Wang [8] assumed that the thermal conductivity can be modeled by taking into account the water thermal conductivity, the interaction between the solvent ($\Delta\lambda^s$) and ion species, the interaction between two ion species ($\Delta\lambda^{s-s}$).

$$\lambda_{elec} = \lambda_{water}(T) + \Delta\lambda^s + \Delta\lambda^{s-s} \quad (35)$$

For our binary system (NaOH, KOH-H_2O), the previous model becomes:

$$\lambda_{elec} = \lambda_{water}(T) + X_i (\alpha_{1i} + \alpha_{2i} \exp(-AT)) + X_k (\alpha_{1k} + \alpha_{2k} \exp(-AT))) (\beta_1 \exp(\beta_2 T)) X_k X_i) \quad (36)$$

for KOH i=K^+ k=OH^-, for NaOH i=Na^+, k=OH^- A=-0.023

6.2.3 KOH

For the KOH, data are available in the range T in [0;155°C] and Y_{KOH} in [0;0.40] of KOH mass fraction. The thermal conductivity increases with temperature but decreases with mass fraction. The sensitivity with respect to the mass fraction and temperature is of the same order of magnitude. The two chosen models are Zaytsev's [3] eq. (34) and Wang's eq. (35) model [15]. Zaytsev's model [3] is valid for T in [20;115°C] and Y_{KOH} in [0;0.40] and it deviate from its experimental data about 1.5% on average with a maximum of 4.4% at 115°C and 0.2 in mass. Wang [15] does not report the values of the coefficient for his model for KOH but they have been identified. The resulting model is valid in the range T in [60;100]°C and Y_{KOH}=[0.02;0.40]. It deviates of 0,47% with a maximum of 2.8% comparing with Zaytsev's data and 1% in average with a maximum of 3.25% with Riedel's data.

6.2.4 NaOH

The data available in Zaytsev [3] are for T in [0;155]°C and Y_{NaOH} in [0;0.35]. The correlation given by Zaytsev eq. (34) is accurate for T=[20-115°C] and Y_{NaOH} in [0.05;0.35] with an average difference of 4.92% and a maximum 12.04% at 20°C and 0.35 NaOH mass fraction. The original correlation given by Wang [8] eq. (35) has an average difference of 10% with the Zaytsev's data and reaches a maximum of 35% for T=40°C and Y_{NaOH}=0.35. However, after using a minimization method, another

interaction parameter was found. By replacing the original parameters by the new one, the average difference falls to 3% and the maximum with a maximum of 6% for T=40°C and Y_{NaOH} =0.35.

Table 8 and figure 8 around here

7 Mass transfer: mass transfer coefficient

The ternary charge distribution shows a limit in current density. This limit is governed by mass transfer. Indeed the limit current density is dependent on the coefficient of diffusion, the hydrodynamic/mass transfer and the bulk concentration of active species eq. (37).

$$j_L = z\ F\ D\ C_{bulk}\ \delta^{-1} = z\ F\ k\ C_{bulk} \quad (37)$$

The coefficient D must be known. The data given by Zaytsev [3] are sparse and are presented on the form of D_{KOH} . This means that the ions OH^- and K^+/Na^+ respect the electroneutrality which is true in the bulk but not true near the electrodes ue to the presence of the layer of negative charge.

7.1 Multilinear interpolation

Zaytsev [3] does not give correlations modelling the diffusion coefficient and the data for NaOH were rare. However, a bilinear interpolation has been developed to model the evolution of this parameter for NaOH and KOH. Nevertheless, due to the lack of data for NaOH the model must be used bearing in mind that it is an extrapolation of few data points.

$$D(Y_i,T) = K_1 + K_2\ Y + K_3\ T + K_4\ T\ Y \quad (38)$$

Table 9 and figure 9 around here

8 Conclusion

All the parameters for simulating with accuracy the alkaline water electrolysis using CFD has been compiled. In addition to the values and correlations found in the literatures, additional correlations has been developed. However, it must be reminded that this model is monophasic whereas real electrolysis is at least biphasic due to the presence of H_2 and O_2 bubbles and further work must be performed in order to review thermal, electro-kinetic parameter and transfer properties of electrode material.

Acknowledgement

We would like to thank the national association ADEME, the French Brittany Region and the company ARMOR MECA for funding our research.

References

[1] Prasad Prakash Patel, Oleg. I. Velikokhatnyi, Shrinath D. Ghadge, Prashanth J. Hanumantha, Moni Kanchan Datta, Kuruba R, et al. Electrochemically active and robust cobalt doped copper phosphosulfide electro-catalysts for hydrogen evolution reaction in electrolytic and photoelectrochemical water splitting. Int J Hydrog Energy 2018;43:7855–71. doi:10.1016/j.ijhydene.2018.02.147.

[2] Prasad Prakash Patel, Prashanth Jampani Hanumantha, Moni Kanchan Datta, Oleg I. Velikokhatnyi, Daeho Hong, Poston JA, et al. Cobalt based nanostructured alloys: Versatile high performance robust hydrogen evolution reaction electro-catalysts for electrolytic and photo-electrochemical water splitting. Int J Hydrog Energy 2017;42:17049–62. doi:10.1016/j.ijhydene.2017.05.175.
[3] Zaytsev. Properties of Aqueous Solutions of Electrolytes. CRC Press 1992. https://www.crcpress.com/Properties-of-Aqueous-Solutions-of-Electrolytes/Zaytsev-Aseyev/p/book/9780849393143 (accessed September 13, 2017).
[4] Dawn M. See, Ralph E. White. Temperature and Concentration Dependence of the Specific Conductivity of Concentrated Solutions of Potassium Hydroxide. J Chem Eng Data 1997;42:1266–8. doi:10.1021/je970140x.
[5] V. P. Mashovets, I. A. Dibrov, B. S. Krumgal'z, R. P. Matveeva. Density of Aqueous KOH solutions at high temperature over a wide range of concentrations. J Appl Chem USSR 1965;38.
[6] L. B. Hitchcock, J. S. McIlhenny. Viscosity and density of pure alkaline solutions and their mixtures. Ind Eng Chem 1935;27.
[7] J Krey. Vapor-pressure and density of system H2O-NaOH. Z Phys Chem-Frankf 1972;81:252.
[8] I. N. Maksimova, V. F. Yushkevich. Electroconductivity of NaOH solutions at high temperatures. Zhurnal Fiz Khimii 1963;37:903–7.
[9] W. Krings. The viscosity and density of sodium hydroxide solutions to high concentrations and at high temperatures. Z Anorg Chem 1948;255:294.
[10] R Gilliam, J Graydon, D Kirk, S Thorpe. A review of specific conductivities of potassium hydroxide solutions for various concentrations and temperatures. Int J Hydrog Energy 2007;32:359–64. doi:10.1016/j.ijhydene.2006.10.062.
[11] M. A. Klochko and M. M. Godneva. Electrical conductivity and viscosity of aqueous solutions of NaOH and KOH. Russ J Inorg Chem 1959;4:964–7.
[12] Y. Guo et al. Density and viscosity of aqueous solution of K2CrO4/KOH mixed electrolytes. Trans Nonferrous Met Soc China 2010;20:32–6.
[13] M. Laliberté. A Model for Calculating the Heat Capacity of Aqueous Solutions, with Updated Density and Viscosity Data. J Chem Eng Data 2009;54:1725–60.
[14] A. H. Roux et al. Capacites calorifiques, volumes, expansibilites et compressibilites des solutions aqueuses concentrees de LiOH, NaOH et KOH. Can J Chem n.d.;62:878–85.
[15] P. Wang, A. Anderko. Modeling Thermal Conductivity of Concentrated and Mixed-Solvent Electrolyte Systems. Ind Eng Chem Res 2008;47:5698–709.
[16] L. Riedel. Die Wärmeleitfähigkeit von wäßrigen Lösungen starker Elektrolyte. Chem Ing Tech 1951;23:59–64.
[17] G. Akerlof, G. Kegeles. The Density of Aqueous Solutions of Sodium Hydroxide. J Am Chem Soc 1939;61:1027–32.
[18] J. Olsson, A. Jernqvist, G. Aly. Thermophysical Properties of Aqueous NaOH-H2O Solutions at High Concentrations. Int J Thermophys 1996;18:779–94.
[19] A. V. Churikov and al. Density Calculations for (Na, K)BH4 + (Na, K)BO2 + (Na, K)OH + H2O Solutions Used in Hydrogen Power Engineering. J Chem Eng Data 2011;56:3984–93.
[20] Victor MM Lobo, JL Quaresma. Handbook of electrolyte solutions. vol. 41. Elsevier; 1989.
[21] P. Olivier and al. Low-temperature electrolysis system modelling : a review. Renew Sustain Energy Rev 2017;78:280–300.
[22] S. D. Hamann and M. Linton. Electrical Conductivities of Aqueous Solutions of KCl, KOH and HCl, and the Ionization of Water at High Shock Pressures. Trans Faraday Soc 1969;65:2186–96.
[23] A. B. Gancy, S. B. Brummer. Conductance of Aqueous Electrolyte Solutions at High Pressures. J Chem Eng Data 1971;16:385–8.
[24] R. A. Fine and F. J. Millero. Compressibility of water as a function of temperature and pressure. J Chem Phys 1973;59:5529–35.
[25] B. Le Neindre. Effet de la pression sur la viscosité des fluides. Tech Ing 2006.
[26] J. W. P Schmelzer and al. Pressure dependdence of viscosity. J Chem Phys 2005;122.

[27] B. Le Neindre. Conductivité thermiques des fluides sous pression. Tech Ing 1999.
[28] Frank Allebrod, Christodoulos Chatzichristodoulou, Pia Lolk Mollerup, Mogens Bjerg Mogensen. Electrical conductivity measurements of aqueous and immobilized potassium hydroxide. Int J Hydrog Energy 2012;37:16505–14. doi:10.1016/j.ijhydene.2012.02.088.
[29] Gosta Akerlof, Paul Bender. The Density of Aqueous Solutions of Potassium Hydroxide. J Am Chem Soc 1941;63:1085–8. doi:10.1021/ja01849a054.

9 Figure

Figure 1-Top: Simulated normalized intensity evolution depending on the tension of the cell according to the three types of model. Bottom : Evolution of the local temperature, mass fraction and velocity near an electrode

Figure 2-Up: Boiling point of the two electrolytes depending on their local mass fraction, black dot are for KOH boiling point and grey for NaOH boiling point. Bottomt: the saturated vapor pressure of the two electrolytes depending on the local temperature and with a sensitivity of 6% for the local mass fraction. Black is for KOH and grey for NaOH.

Figure 3-Illustration of the comparison methodology

Figure 4- Electrical conductivity of KOH and NaOH depending on temperature and mass fraction. For both KOH and NaOH, triangle represents experimental data from Zaytsev [3]. For KOH (left) the dotted line is the correlation from Gilliam [10] and the solid line is the correlation from See [4]. For NaOH (right) the dotted line represents the correlation from [12]. For temperature sensitivity (top), black is for Yk=36%(KOH°, 22%(NaOH) and grey for 30% (KOH) 20% (NaOH). For concentration sensitivity, grey is for 75°C and black 85°C

Figure 5-Density of KOH and NaOH depending on temperature and mass fraction. For both KOH and NaOH, triangle and the solid line represents the experimental point and their correlation of Zaytsev [3]. For KOH (left), the cross symbol is for Mashovets data, the dotted line is the correlation from Gilliam [10]. For NaOH (right) the dotted line represents the correlation from Churikov [19]. For temperature sensitivity (top), black is for Y=0.36KOH, 0.22NaOH and grey for 0.3 (KOH) 0.2 (NaOH). For concentration sensitivity, grey is for 75°C and black 85°C.

Figure 6- Viscosity of KOH and NaOH depending on temperature and mass fraction. For both KOH and NaOH, triangles and the solid lines represent the experimental point and their correlation of Zaytsev [3]. For KOH (left), the cross symbol is for Hitchcock data, the dotted line is the correlation from Guo [12]. For NaOH (right), the square symbol is for Kring's data, the dotted line represents the correlation from Olsson [18]. For temperature sensitivity (top), black is for Y=0.36(KOH°, 0.22(NaOH) and grey for 0.30 (KOH) 0.20 (NaOH). For concentration sensitivity, grey is for 75°C(KOH) 70°C(NaOH) and black 85°C(KOH) 80°C(NaOH).

Figure 7- Specific heat of KOH and NaOH depending on temperature and mass fraction. For both KOH and NaOH, triangles and the solid line represent the experimental point and their correlation of Zaytsev [3]. For KOH (left) and NaOH the dotted line is the correlation determined using method from Laliberté [13]. For temperature sensitivity (top), black is for Y=0.36(KOH°, 0.22(NaOH) and grey for 0.30 (KOH) 0.20 (NaOH). For concentration sensitivity, grey is for 75°C(KOH) 70°C(NaOH) and black 85°C(KOH) 80°C(NaOH

Figure 8-Thermal conductivity of KOH and NaOH depending on temperature and mass fraction. For both KOH and NaOH, triangles and the solid line represent the experimental point and their correlation of Zaytsev [3], the dotted line is the correlation from [15] and the dotted line is a modified correlation using Wang [15]. For KOH, the cross symbol is for Riedel data [16]. For temperature sensitivity (top), black is for Y=0.36 and grey for 0.30. For concentration sensivity (bottom), grey is for 75°C and black 85°C.

Figure 9 Diffusion coefficient of KOH and NaOH depending on temperature and mass fraction. For both KOH and NaOH, triangle are data from Zaytsev and solid line are LeBideau's model.

10 Table

Table 1-Summary of the references depending on their works

Table 2-Constants for electrical conductivity correlations the equations are evaluated for T in [40;70]°C and Y in[0.16;0.32] for KOH.and for T in [25;50]°C and Y in [0.08;0.25]. Z is for Zaytsev et al [3] and S for See et al [4]

Table 3-Comparison between model of density. The comparison has been performed over Y in [0.02-0.4] and T in [60-100]°C for KOH and Y in [0.02-0.22] and T in [60-100]°C for NaOH. MH is for Mashovets,

Table 4-Parameter for Olson's correlation [11]

Table 5-Domain of validity of the Olsson's correlation [11]

Table 6-Comparison of viscosity model. Comparison has been performed T in [40;100]°C and Y in [0;0.4] H is for Hitchcock [6] and KR is for Krings [9]

Table 7-Comparison of different specific heat correlation. The comparison has been performed T in [60;100]°C for Zaytsev data and [25;55]°C for Roux data for NaOH and KOH and Y in [0;0.4] for KOH and [0;0.2] for NaOH

Table 8-Parameters thermal conductivity model

Table 9-Parameters for the Multilinear interpolation to calculate the mass transfer coefficient

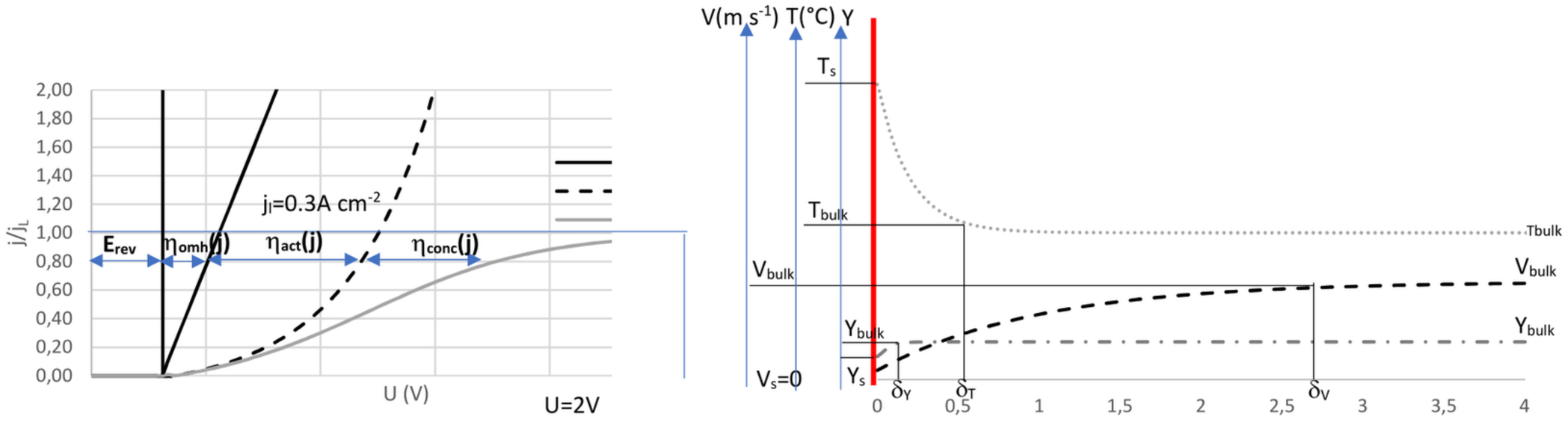

Figure 1-Top: Simulated normalized intensity evolution depending on the tension of the cell according to the three types of model. Bottom : Evolution of the local temperature, mass fraction and velocity near an electrode

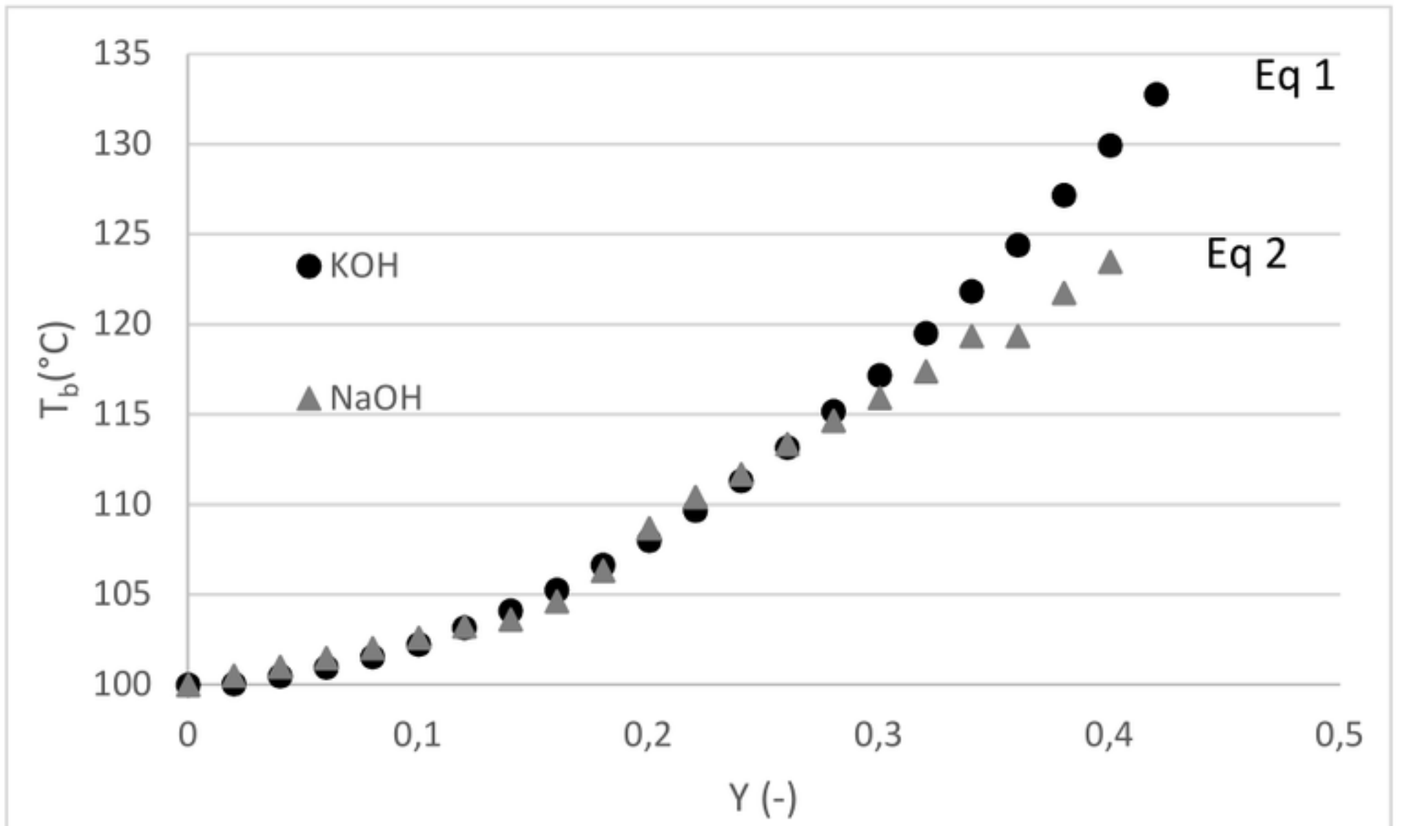

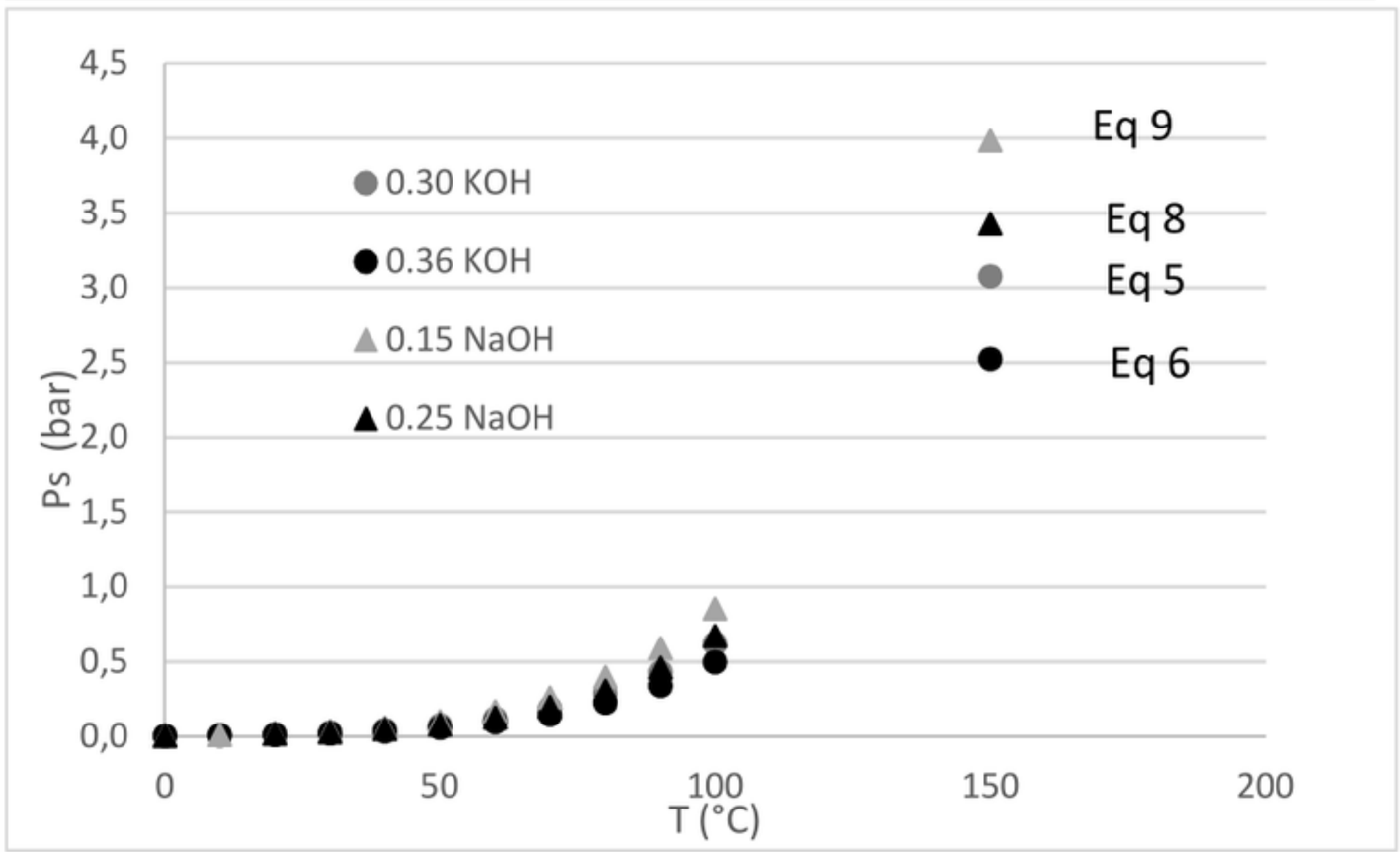

Figure 2-Up:Boiling point of the two electrolytes depending on their local mass fraction, black dot are for KOH boiling point and grey for NaOH boiling point. Bottomt: the saturated vapor pressure of the two electrolytes depending on the local temperature and with a sensitivity of 6% for the local mass fraction. Black is for KOH and grey for NaOH.

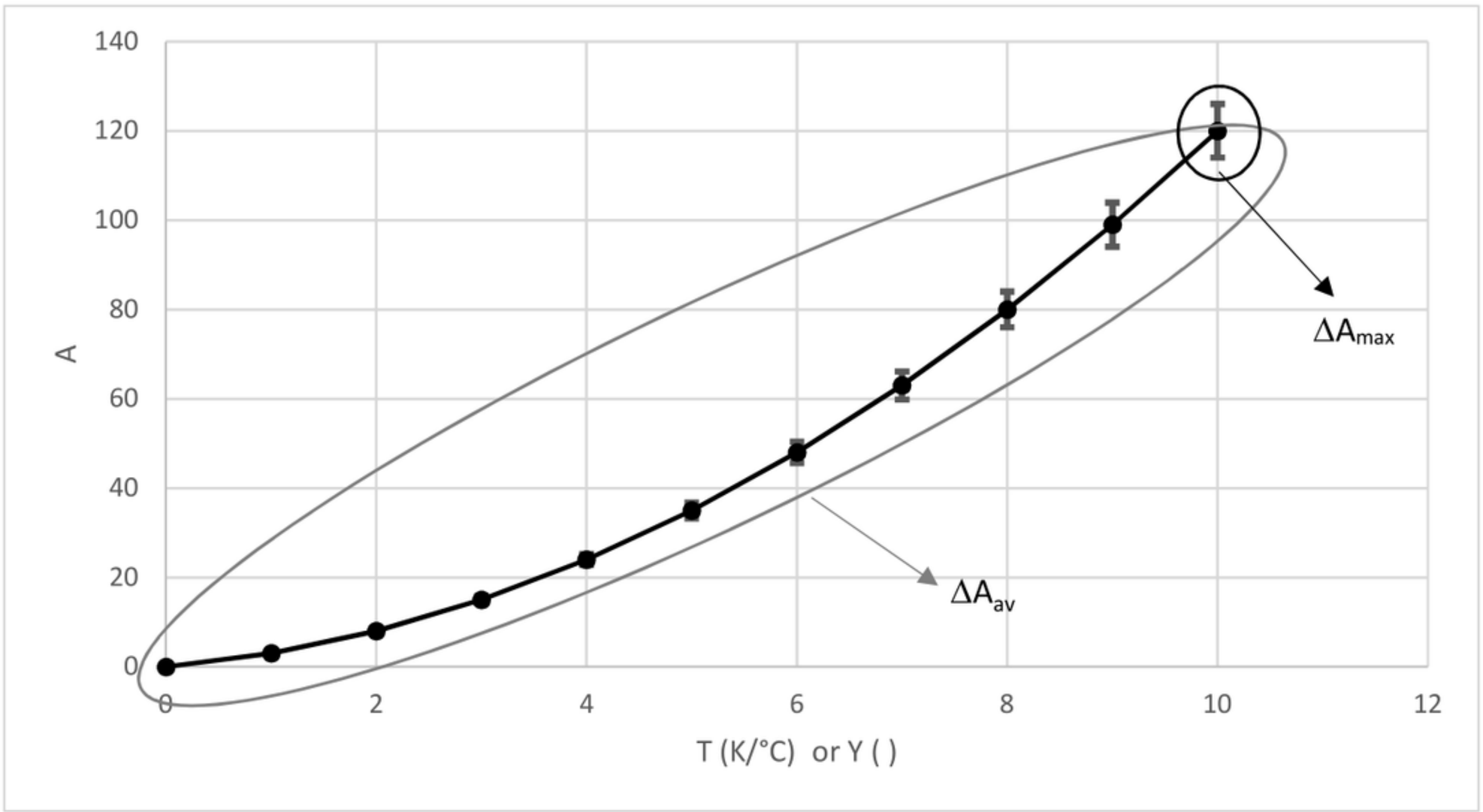

Figure 3-Illustration of the comparison methodology

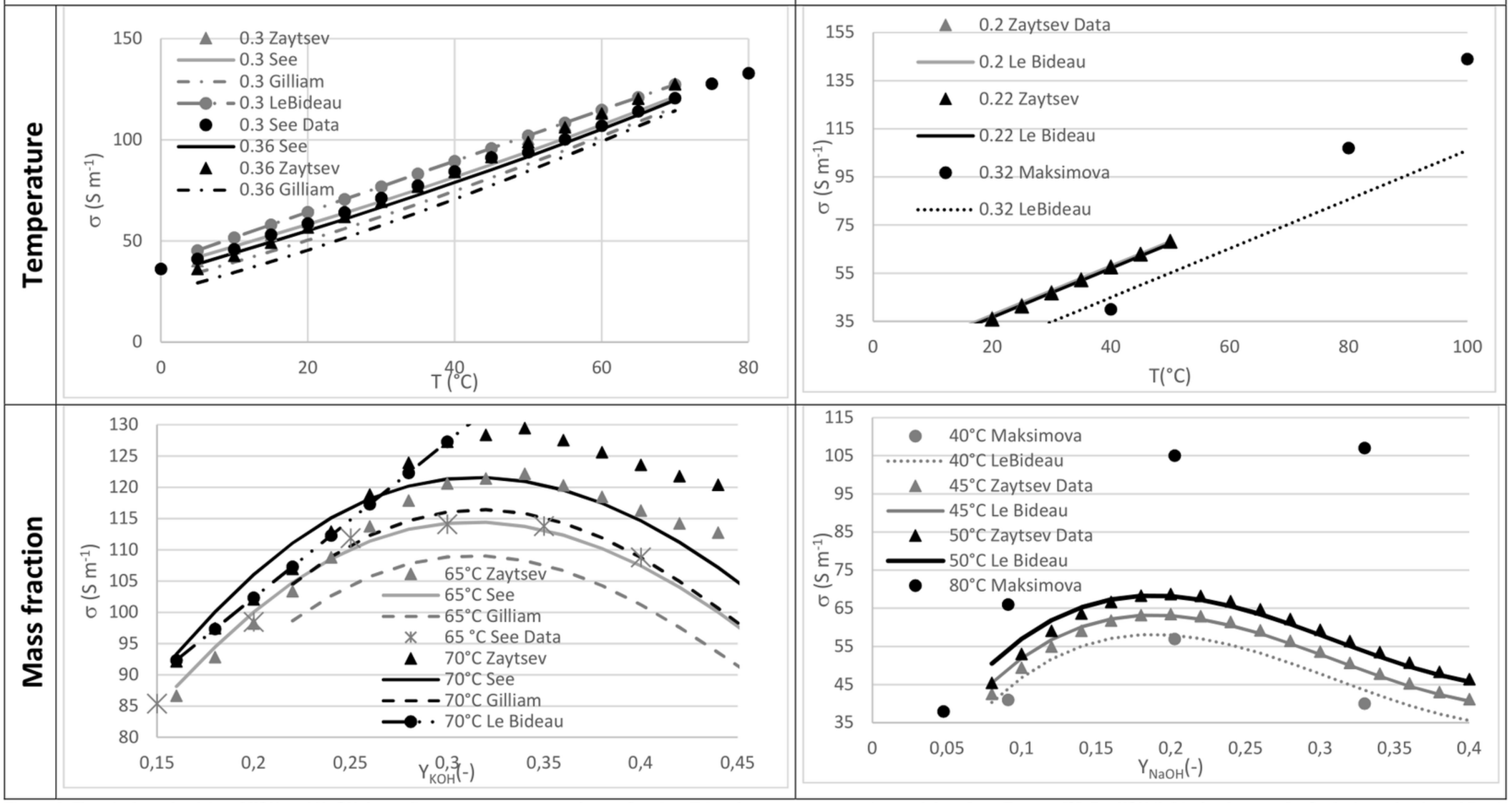

Figure 4- Electrical conductivity of KOH and NaOH depending on temperature and mass fraction. Triangle represents experimental data from Zaytsev [3]. For KOH (left), the dots are for See's data, the dotted line is the correlation from Gilliam [10] and the solid line is the correlation from See [4]. For NaOH (right), the dots are for Maksimova's data, the dotted line represents the correlation from this study. For temperature sensitivity (top), black is for Y=0.36 (KOH), 0.22 (NaOH) and grey for 0.30 (KOH), 0.20 (NaOH). For concentration sensitivity, grey is for 75°C and black 85°C.

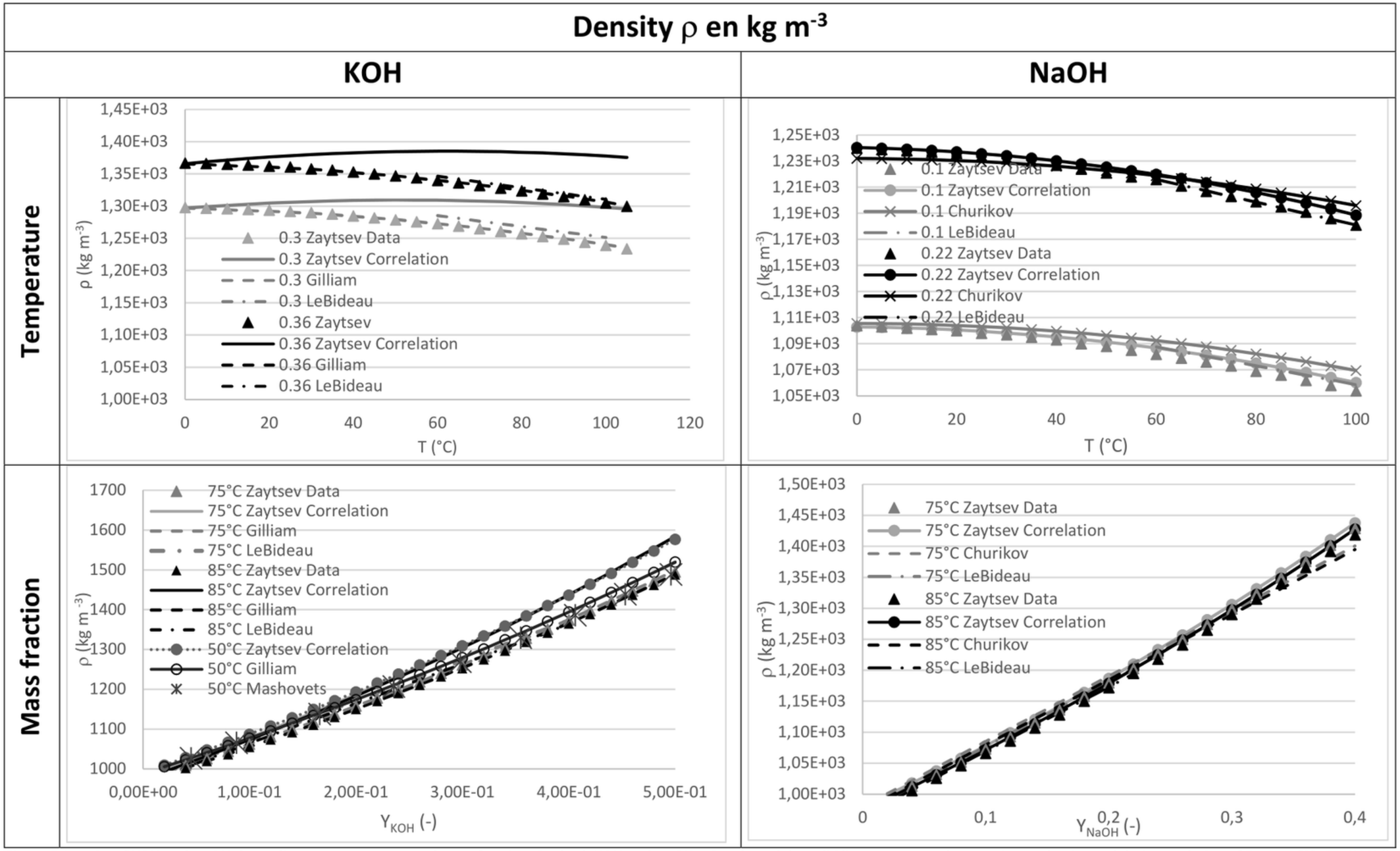

Figure 5-Density of KOH and NaOH depending on temperature and mass fraction. For both KOH and NaOH, triangle and the solid line represents the experimental point and their correlation of Zaytsev [3]. For KOH (left), the cross symbol is for Mahsovets data, the dotted line is the correlation from Gilliam [10]. For NaOH (right) the dotted line represents the correlation from Churikov [19]. For temperature sensitivity (top), black is for Y=0.36KOH, 0.22NaOH and grey for 0.3 (KOH) 0.2 (NaOH). For concentration sensitivity, grey is for 75°C and black 85°C.

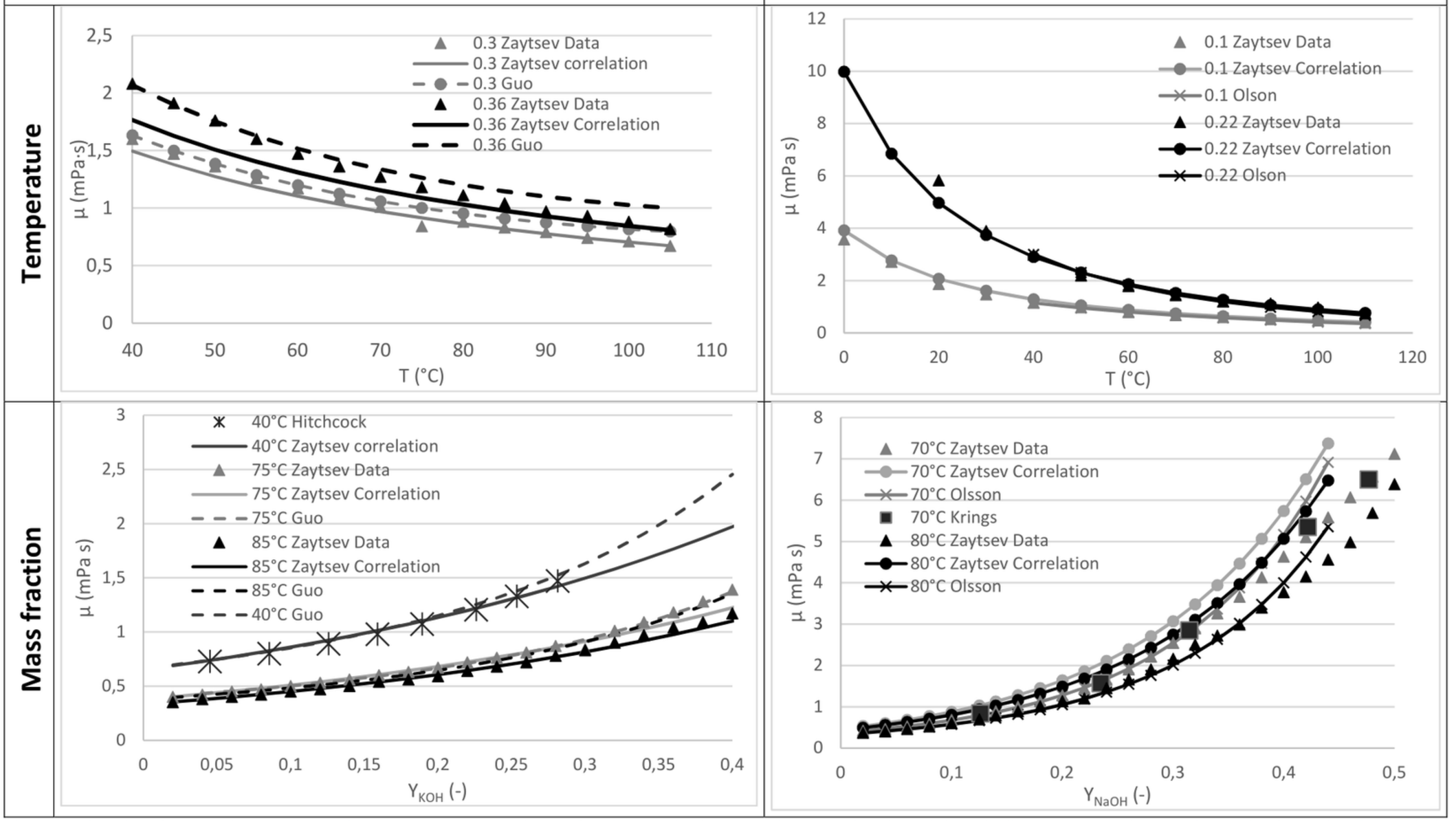

Figure 6- Viscosity of KOH and NaOH depending on temperature and mass fraction. For both KOH and NaOH, triangle and the solid line represents the experimental point and their correlation of Zaytsev [3]. For KOH (left), the cross symbol is for Hitchcock data, the dotted line is the correlation from Guo [12]. For NaOH (right), the square symbol is for Kring's data, the dotted line represents the correlation from Olsson [18]. For temperature sensitivity (top), black is for Y=0.36(KOH°, 0.22(NaOH) and grey for 0.30 (KOH) 0.20 (NaOH). For concentration sensitivity, grey is for 75°C(KOH) 70°C(NaOH) and black 85°C(KOH) 80°C(NaOH).

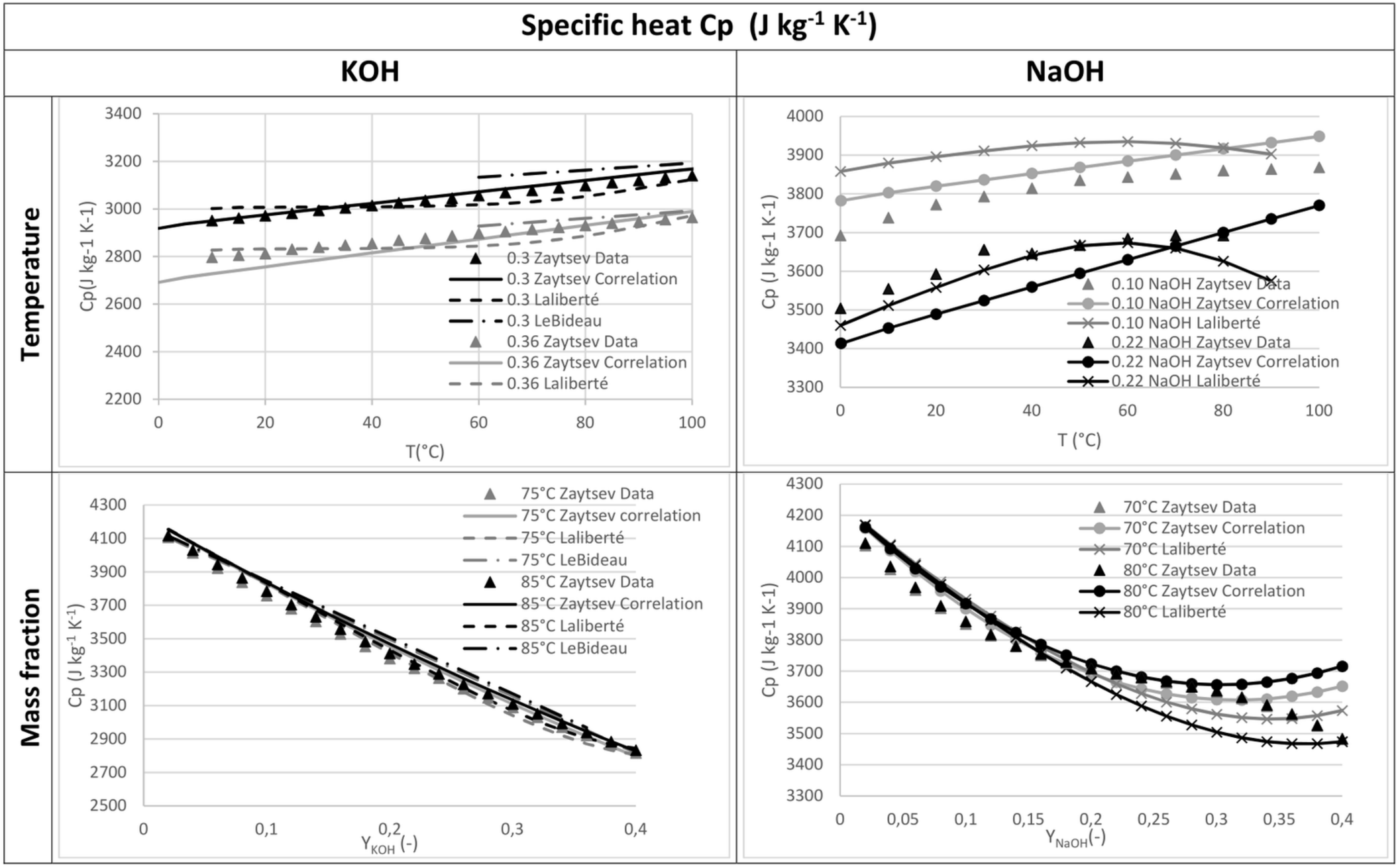

Figure 7- Specific heat of KOH and NaOH depending on temperature and mass fraction. For both KOH and NaOH, triangle and the solid line represents the experimental point and their correlation of Zaytsev [3]. For KOH (left) and NaOH the dotted line is the correlation determined using method from Laliberté [13]. For temperature sensitivity (top), black is for Y=0.36(KOH°, 0.22(NaOH) and grey for 0.30 (KOH) 0.20 (NaOH). For concentration sensitivity, grey is for 75°C(KOH) 70°C(NaOH) and black 85°C(KOH) 80°C(NaOH)

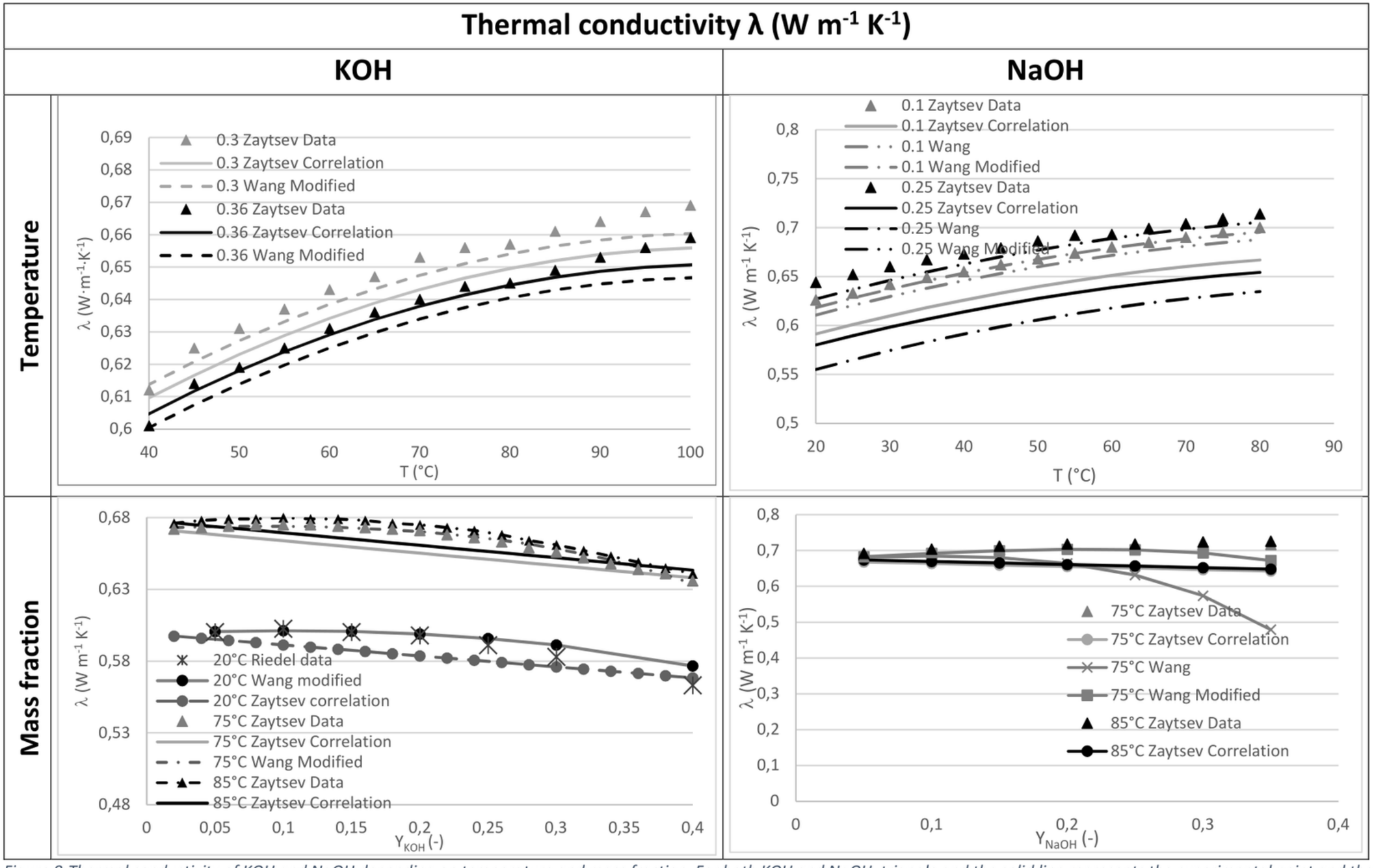

Figure 8-Thermal conductivity of KOH and NaOH depending on temperature and mass fraction. For both KOH and NaOH, triangle and the solid line represents the experimental point and their correlation of Zaytsev [3], the cross symbol is for Riedel data[16] , the dotted line is the correlation from [15] and the dotted line is a modified correlation using Wang [15]. For temperature sensitivity (top), black is for Y=0.36 and grey for 0.30. For concentration sensivity (bottom), grey is for 75°C and black 85°C.

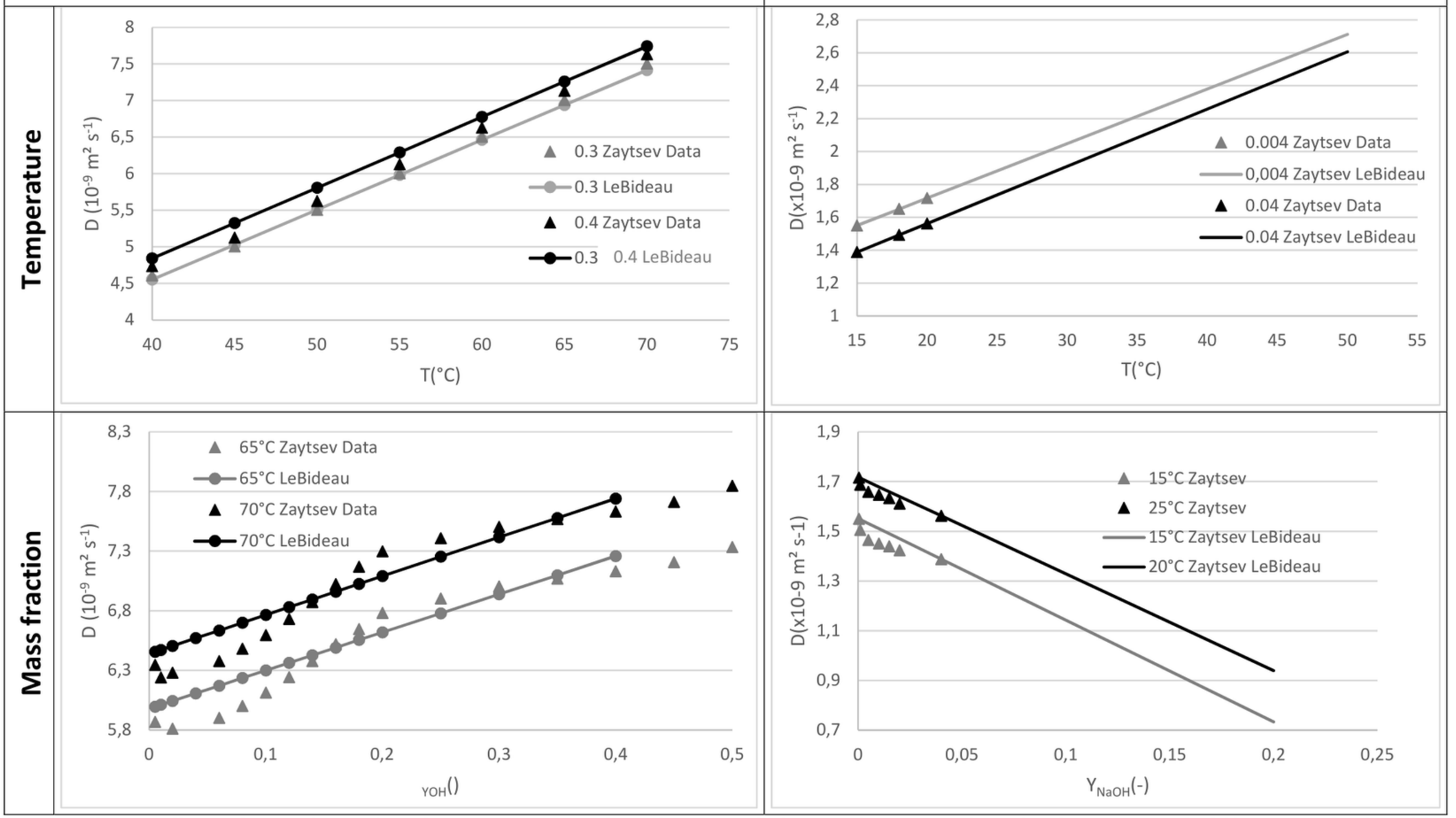

Figure 9 Diffusion coefficient of KOH and NaOH depending on temperature and mass fraction. For both KOH and NaOH, triangle are data from Zaytsev and solid line are LeBideau's model. For KOH, black is 70°C and 0.4 mass fraction, grey is 65°C and 0.3 mass fraction. For NaOH, black is 25°C and 0.04 mass fraction and grey is for 15°C and 0.004 mass fraction.

Table 1-Summary of the references depending on their works

	Electrical Cond.								Density								Viscosity								Specific Heat								Thermal Cond.								Diffusivity Coef.							
	KOH				NaOH				KOH				NaOH				KOH				NaOH				KOH				NaOH				KOH				NaOH				KOH				NaOH			
	T		Yk		T		Yk		T		Yk		T		Yk		T		Yk		T		Yk		T		Yk		T		Yk		T		Yk		T		Yk		T		Yk		T		Yk	
	D	C	D	C	D	C	D	C	D	C	D	C	D	C	D	C	D	C	D	C	D	C	D	C	D	C	D	C	D	C	D	C	D	C	D	C	D	C	D	C	D	C	D	C	D	C	D	C
Zaytsev et al[3]	X		X		X		X		X	X	X	X	X	X	X	X	X	X	X	X	X	X	X	X	X	X	X	X	X	X	X	X	X	X	X	X	X	X	X	X	X		X		X		X	
See et al [4]	X	X	X	X																																												
Gilliam et al [10]	X	X	X	X					X	X	X	X																																				
Klochko et al [11]	X		X		X		X										X		X		X		X																								
Guo et al [12]									X	X	X	X					X	X	X	X																												
Laliberté [13]										X		X		X		X		X		X		X		X		X		X				X															
Roux et al [14]																									X		X	X	X		X	X															
Wang et al [15]																																		X		X		X		X							
Riedel et al [16]																																		X	X	X		X	X	X							
Akerlof et al [17]													X	X	X	X																															
Olsson et al [18]													X	X	X	X					X	X	X	X																							
Churikov et al [19]									X	X	X	X	X	X	X	X																															
Lobo et al [20]	x		x		x		x		x		x		x		x		x		x		x		x																		x		x		x		x	
Maksimova et al[8]					x		x																																									
Krey [7]													x		x																																	
Mashovets et al[5]	x		x																																												
Krings et al[9]													x		x						x		x																								
Hitchcock et al [6]																	x		x																												
Le Bideau et al	X	X	X	X	X	X	X	X	X	X	X	X	X	X	X	X	X	X	X	X	X	X	X	X	X	X	X	X	X	X	X	X	X	X	X	X	X	X	X	X	X	X	X	X	X	X	X	X

Table 2-Constants for electrical conductivity correlations the equations are evaluated for T in [40;70]°C and Y in[0.16;0.32] for KOH.and for T in [25;50]°C and Y in [0.08;0.25]. Z is for Zaytsev et al [3] and S for See et al [4]

	K_1	K_2	K_3	K_4	K_5	K_6	K_7	K_8	$\Delta\sigma$	$\Delta\sigma_{max}$	Validity range
See et al [4]	$2.80\ 10^{3}$	$-9.241\ 10^{-1}$	$-1.497\ 10^{-2}$	-9.052	$2.591\ 10^{-2}$	$1.765\ 10^{-1}$	$6.966\ 10^{-2}$	$-2.898\ 10^{1}$	Z:4.63% S:1.25%	Z:11.58% S:7.40%	-15-100°C 0.15-0.45
Gilliam et al [10]	2.041	$2.800\ 10^{-3}$	$5.332\ 10^{-3}$	$2.072\ 10^{2}$	$1.043\ 10^{-3}$	$3.000\ 10^{-6}$			Z:5.88% S:3.04%	Z:10.71% S:14.16%	0-100°C 10^{-3}-0.45
LeBideau KOH	$3.899\ 10^{1}$	$1.914\ 10^{-1}$	$9.993\ 10^{-3}$	$2.208\ 10^{-1}$	3.564				Z:3.34% S:15%	Z:18.83% S:49%	40-70°C 0.16-0.32
LeBideau NaOH	$-4.57\ 10^{1}$	1.02	$3.20\ 10^{3}$	$-2.99\ 10^{3}$	$7.84\ 10^{2}$				Z:1.5% MK:20%	Z:11.7% MK:28%	25-50°C 0.08-0.25

Table 3-Comparison between model of density. The comparison has been performed over Y in [0.02;0.4] and T in [60;100]°C for KOH and Y in [0.02;0.22] and T in [60;100]°C for NaOH. MH is for Mashovets,[5]

	K_1	K_2	K_3	K_4	K_5	T	Y_i	$\Delta\rho_{av}$	$\Delta\rho_{max}$
Zaytsev KOH [3]	$1\ 10^{3}$	$6.20\ 10^{-3}$	$-3.55\ 10^{-3}$	$3.76\ 10^{-1}$	$5.94\ 10^{-4}$	0-200°C	0-0.5	Z:<1% MH:2.38%	MH:8.60%
Gilliam et al KOH [10]	$-3.25\ 10^{-3}$	$1.11\ 10^{-1}$	$1.00171\ 10^{3}$	$8.6\ 10^{-1}$		0-200°C	0-0.5	Z:<1% MH:<1%	
Le Bideau KOH	$1.02\ 10^{3}$	$1.06\ 10^{3}$	$-6.09\ 10^{-1}$	$-7.89\ 10^{-1}$		60-100°C	0.02-0.40	Z:0.78% MH:1.22%	Z:1.33% MH:2.42%
Zaytsev NaOH [3]	$1\ 10^{3}$	$6.20\ 10^{-3}$	$-3.55\ 10^{-3}$	$4.25\ 10^{-1}$	$-1.15\ 10^{-4}$	0-200°C	0-0.5	Z:<1% KR:2.16%	Z:0.66% KR:6.84%
Churikov et al NaOH [19]	$1\ 10^{3}$	$6.2\ 10^{-3}$	$-3.55\ 10^{-3}$	$-1\ 10^{1}$	$1.057\ 10^{3}$	0-50°C	0-0.5	Z:1% KR<1%	KR:1.53%
Le Bideau NaOH	$1.02\ 10^{3}$	$1.15\ 10^{3}$	$-6\ 10^{-1}$	-1.25		60-100°C	0.02-0.22	Z:0.25% KR<1%	Z:0.54% KR:1%

Table 4-Parameter for Olsson's correlation [18]

k_1	-6.14	l_1	2.32	m_1	$-1.152\ 10^{-1}$	n_0	$5.87\ 10^{-1}$
k_2	$1.25\ 10^{2}$	l_2	$-2.3\ 10^{1}$	m_2	1.05	n_1	$-3.98\ 10^{-1}$
k_3	$-2.47\ 10^{2}$	l_3	$4.93\ 10^{1}$	m_3	-2.37	n_2	$2.47\ 10^{-3}$
k_4	$1.47\ 10^{2}$	l_4	$-3.697\ 10^{1}$	m_4	2.10	n_3	$-4.94\ 10^{-6}$
		l_5	6.58	m_5	$-5.25\ 10^{-1}$	n_4	$1.49\ 10^{-7}$

Table 5-Domain of validity of the Olsson's correlation [18]

Y_{NaOH}	T (°C)
Between 0.02-0.4	20-30°C
Between 0.02-0.45	30-50°C
Between 0.02-0.55	50-70°C
Between 0.02-0.70	70-150°C

Table 6-Comparison of viscosity model. Comparison has been performed T in [40;100]°C and Y in [0;0.4] H is for Hitchcock [6] and KR is for Krings [9]

	K_1	K_2	K_3	K_4	K_5	T	Y_i	$\Delta\mu_{av}$	$\Delta\mu_{max}$
Zaytsev KOH [3]	$5.98\ 10^{-1}$	4.33 10	1.54	1.12	$2.03\ 10^{-3}$	0-200°C	0-0.50	Z:2.9% H:4.8%	Z:18% H:25%
Guo KOH et al [12]	$4.3\ 10^{-1}$	$-2.51\ 10^{-2}$	10^{-4}	$1.3\ 10^{-1}$		20-60°C	0.02-0.4	Z:5% H:2.73%	Z:10% H:7.52%
Zaytsev NaOH[3]	$5.98\ 10^{-1}$	4.33 10	1.54	3.39	$-1.12\ 10^{-2}$	0-200°C	0-0.50	Z:5% KR:8%	KR:30%

Table 7-Comparison of different specific heat correlation. The comparison has been performed T in [60;100]°C for Zaytsev data and [25;55]°C for Roux data for NaOH and KOH and Y in [0;0.4] for KOH and [0;0.2] for NaOH

	K_1	K_2	K_3	K_4	K_5	K_6	T	Y_i	ΔCp_{av}	ΔCp_{max}
Zaytsev KOH [3]	$4.236\ 10^{3}$	1.075	$-4.831\ 10^{3}$	8			0-200°C	0-0.4	Z:2% R:6.27%	Z:8% R:29.8%
Zaytsev NaOH [3]	$4.236\ 10^{3}$	1.075	$1.576\ 10^{3}$	$1.59\ 10^{1}$			0-200°C	0-0.4	2%	4.32%
Laliberté KOH [13]	$1.689\ 10^{1}$	$1.60\ 10^{-5}$	-6.35	$2.039\ 10^{-1}$	$4.045\ 10^{4}$	4.68	60-100°C	0.02-0.4	Z:1.1% R:6.65%	Z:2.58% R:32.7%
Laliberté NaOH [13]	$9.878\ 10^{3}$	$5.644\ 10^{-2}$	-3.143	2.593	$2.174\ 10^{6}$	$-9.310\ 10^{3}$	60-100°C	0.02-0.2	3%	8%
Le Bideau KOH	$4.101\ 10^{3}$	$-3.526\ 10^{3}$	$9.644\ 10^{-1}$	1.776			60-100°C	0.02-0.4	Z:1.79 R:6.13%	4.02% R:27.4%
Le Bideau NaOH	$3.879\ 10^{3}$	$-2.068\ 10^{2}$	$6.63\ 10^{-1}$	$-2.36\ 10^{-1}$			60-100°C	0.02-0.2	1.09%	1.95%

Table 8-Parameters thermal conductivity model

					β_{wang}		$\beta_{LeBideau}$		$\Delta\lambda_{av}$	$\Delta\lambda_{max}$
	α_{1i}/K_1	α_{2i}/K_2	α_{1k}/K_3	α_{2k}/K_4	1	2	1	2		
Zaytsev KOH[3]	$5.545\ 10^{-1}$	$2.460\ 10^{-3}$	$1.184\ 10^{-5}$	$1.280\ 10^{-1}$					Z:1.5% R:1.4%	Z:3% R:6%
Wang KOH[15]	$-3.8249\ 10^{-1}$	$4.49\ 10^{-2}$	$4.923\ 10^{-1}$	$-1.8\ 10^{-2}$	--	--	-1.84	--	Z:0.47% R:1%	Z:2.8% R:3.25%
Zaytsev NaOH[3]	$5.545\ 10^{-1}$	$2.460\ 10^{-3}$	$1.184\ 10^{-5}$	$1.260\ 10^{-1}$					4.92%	12.04%
Wang NaOH[15]	0	0	$4.923\ 10^{-1}$	$-1.8\ 0^{-2}$	-4.95	$-2.5409\ 10^{-4}$	-1.95	$-2.5409\ 10^{-4}$	$10\%_{wang}/3\%_{LeBideau}$	$35\%_{wang}/6\%_{LeBideau}$

Table 9-Parameters for the Multilinear interpolation to calculate the diffusion coefficient

	K_1	K_2	K_3	K_4	T	Y_i	ΔD_{av}	ΔDMax
KOH	$-1.05\ 10^{-1}$	2.45	$9.20\ 10^{-2}$	$1.148\ 10^{-2}$	40-70°C	0.05-0.40	2.24%	5.78%
NaOH	1.05	-4.70	$3.32\ 10^{-2}$	$4.04\ 10^{-2}$	15-20°C	0.004-0.02		